# Electronic supplementary information

## Photophysical Studies for Cu(I)-Based Halides: Broad Excitation Band and Highly Efficient Single-Component Warm White-Light-Emitting Diode

*Shuigen Zhou, Yihao Chen, Kailei Li, Xiaowei Liu, Ting Zhang, Wei Shen, Ming Li, Lei Zhou* and Rongxing He**

*Key Laboratory of Luminescence Analysis and Molecular Sensing (Southwest University), Ministry of Education*

*School of Chemistry and Chemical Engineering, Southwest University, Chongqing 400715, China*

Corresponding Authors: Lei Zhou, Rongxing He

**E-mail addresses:** zhoulei25@swu.edu.cn (L. Zhou), herx@swu.edu.cn (R. He)

## Experimental Section

**Materials:** Cuprous chloride (CuCl, 99%), cuprous bromide and (CuBr, 99%) and cuprous iodide (CuI, 99%) were purchased from Shanghai Aladdin Bio-Chem Technology Co., Ltd (China). Hypophoaphoeous acid ($H_3PO_2$, 50 wt.% in $H_2O$) and acetonitrile ($CH_3CN$, 99%) were purchased from Beijing Innochem Science & Technology Co., Ltd (China). 1,4-Diaminobenzene ($C_6H_8N_2$, 99%) were obtained from Shanghai Macklin Biochemical Co., Ltd (China). All reagents and solvents were used without further purification.

**Synthesis of $DPCu_4X_6$ (X=Cl, Br, I) single crystals:** $DPCu_4X_6$ (X=Cl, Br, I) single crystals were prepared by a same facile hydrothermal method. In short, cuprous halide (0.5 mmol) and $C_6H_8N_2$ (1 mmol) were dissolved in the mixture of acetonitrile (1 mL for $DPCu_4Cl_6$ and $DPCu_4Cl_6$; 3 mL for $DPCu_4I_6$) and hypophoaphoeous acid (1.5 mL) solution at 120 ℃ with constant stirring for 1 h to form a colorless transparent solution. Then, the crystals were obtained by cooling to room temperature with 5 °C/h. The crystals were filtered off, washed with acetonitrile and dried at 40 ℃ for 12 h.

**Structural and spectroscopy characterization：** Single-crystal X-ray diffraction data were collected at 173 K on a Bruker D8 VENTURE diffractometer with Mo Kα radiation, and the structures were resolved and refined by using Shelxt and Olex2. Powder X-ray diffraction (PXRD) data were obtained by using a Bruker D2 PHASER X-ray diffractometer. The hydrogen nuclear magnetic resonance ($^1$H-NMR) spectra were collected on a Bruker AVANCE III 600 MHz NMR spectrometer. The steady-state photoluminescence excitation (PLE) and emission (PL) spectra, temperature-dependent PL/PLE spectra, time-resolved PL decay profiles, photoluminescence quantum yield (PLQY) data and power density-dependent PL spectra were got from a Horiba Jobin Yvon Fluorolog-3 spectrometer. Thermogravimetric analysis was conducted on a TA instruments Q50 TGA system under nitrogen atmosphere at a heating rate of 10 °C min/h to 600 °C. XPS measurements of the samples were conducted on a Thermo K-Alpha spectrometer equipped with a monochromatic Al Kα

X-ray source.

**Computational method：** All the first-principles calculations of $DPCu_4X_6$ (X = Cl, I) were accomplished based on density functional theory (DFT) applying the Vienna *ab-initio* simulation (VASP)[1] code. The interaction between electrons is represented by the augmented wave (PAW)[2] method, the exchange correlation is represented by the Perdew-Burke-Emzerhof (PBE) form of the generalized gradient approximation (GGA)[3], and the cutoff energy was set as 400 eV. Structural geometry optimization was carried out energy convergence of $10^{-6}$ eV and the force convergence on each atom was <0.02 eV/Å. In the Brillouin zone, the k-point spacing is set to 0.04 $Å^{-1}$, resulting in a corresponding Γ-centered k-point grid of 1 × 1 × 1.

**WLED fabrication:** A WLED was fabricated using a blue-GaN chip (~445 nm, San'an Optoelectronics Co., Ltd, China) as the excitation source and $DPCu_4I_6$ as the yellow phosphor. The proper amounts phosphor were mixed with resin (leaftop 9300, Shengzhenshi Tegu New Materials CO., Ltd, China), and the obtained mixture was coated on the chip. The PL spectra, CCT, and CIE color coordinates of the device were tested using OHSP-350M LED Fast-Scan Spectrophotometer (Hangzhou Hopoo Light&Color Technology Co., Ltd, China).

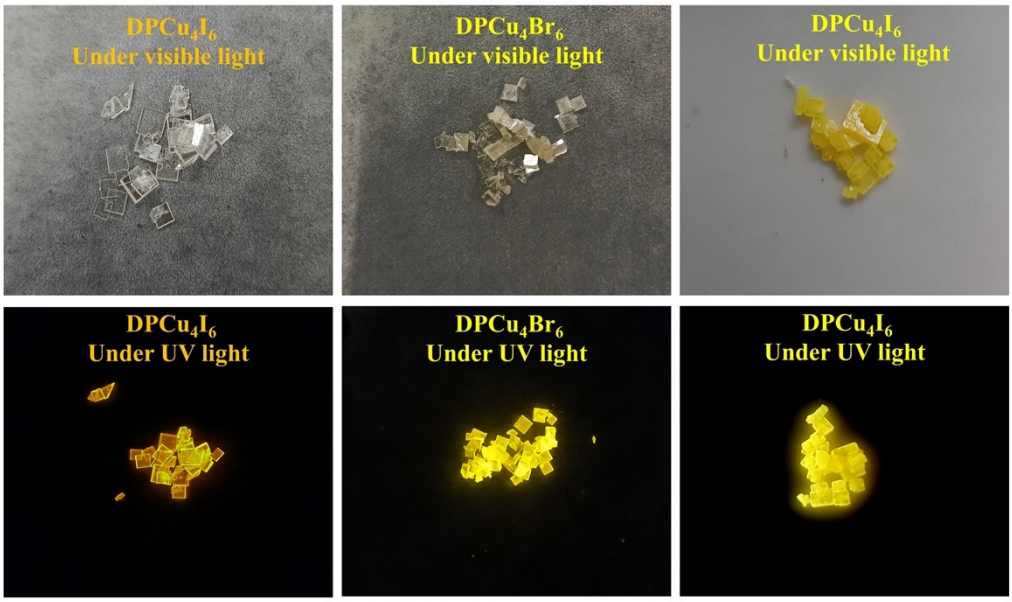


**Figure S1.** Photographs of $DPCu_4X_6$ (X = Cl, Br, I) single crystals under ambient light and 365 nm UV light.

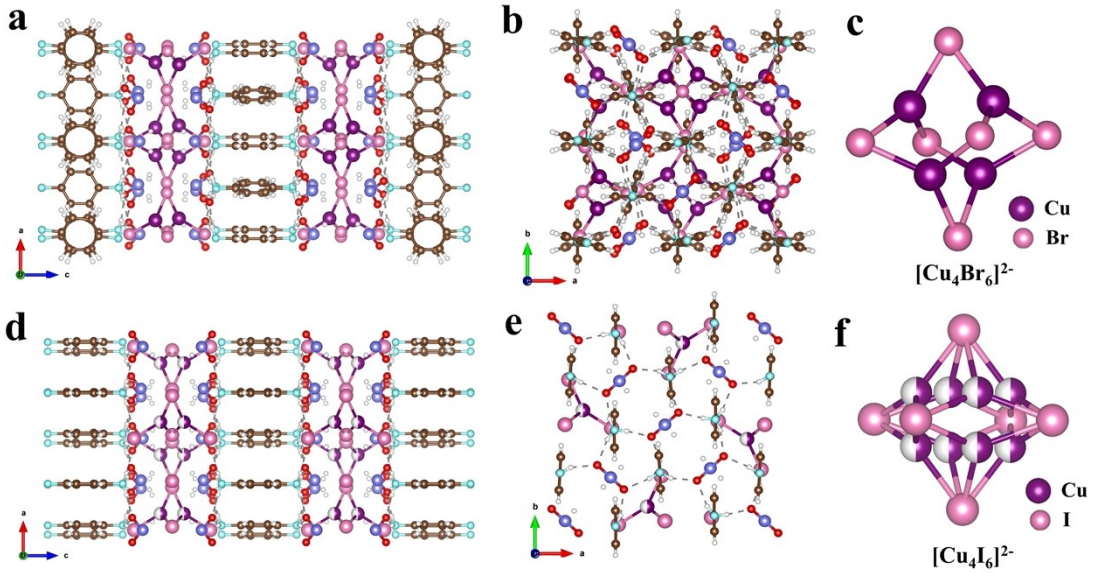


**Figure S2.** Structural information of $DPCu_4X_6$ (X = Br, I) single crystals. Crystal structure of $DPCu_4Br_6$ viewed along the (a) *b* axis and (b) *c* axis (Cu, purple; X, pink; P, blue; O, red; C, brown; N, cyan; H, white). Individual Cu(I)-halogen cluster unit for (c) $DPCu_4Br_6$ and (f) $DPCu_4I_6$. Crystal structure of $DPCu_4I_6$ viewed along the (a) *b* axis and (b) *c* axis.

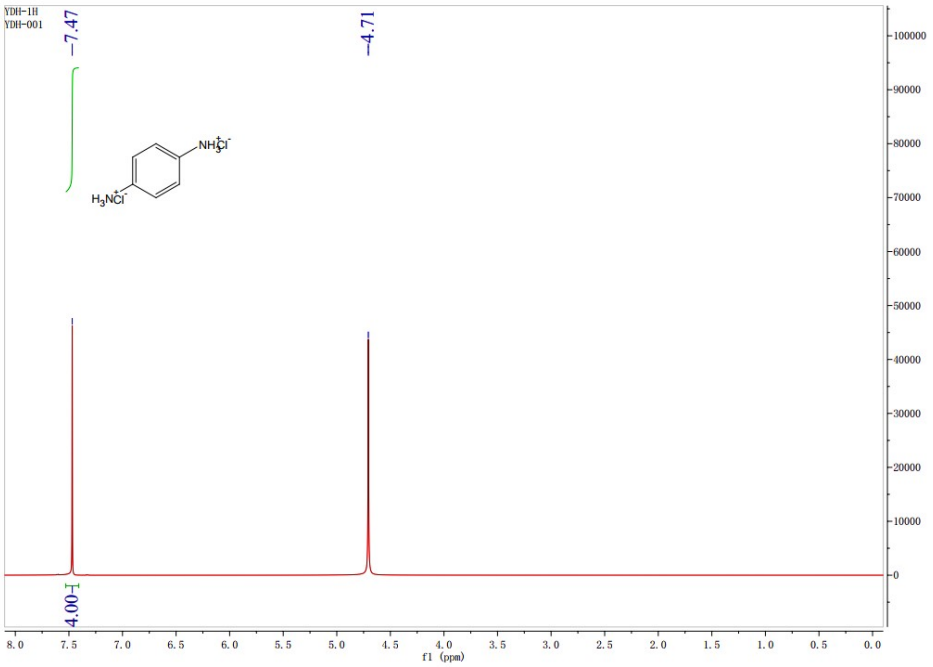


**Figure S3.** $^{1}$H-NMR spectrum of $C_6H_8N_2Cl_2$ measured in $D_2O$.

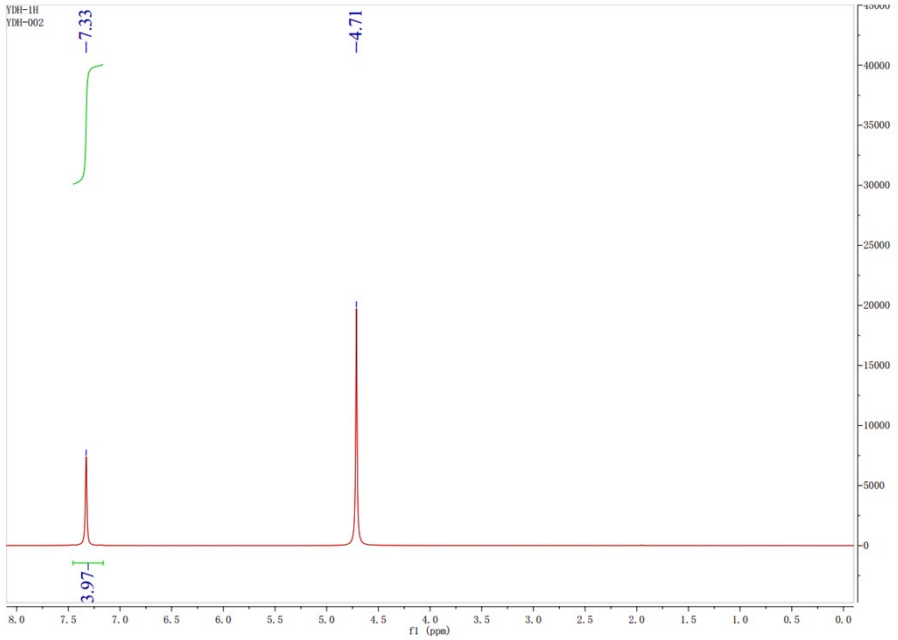


**Figure S4.** $^{1}$H-NMR spectrum of $DPCu_4Cl_6$ measured in $D_2O$.

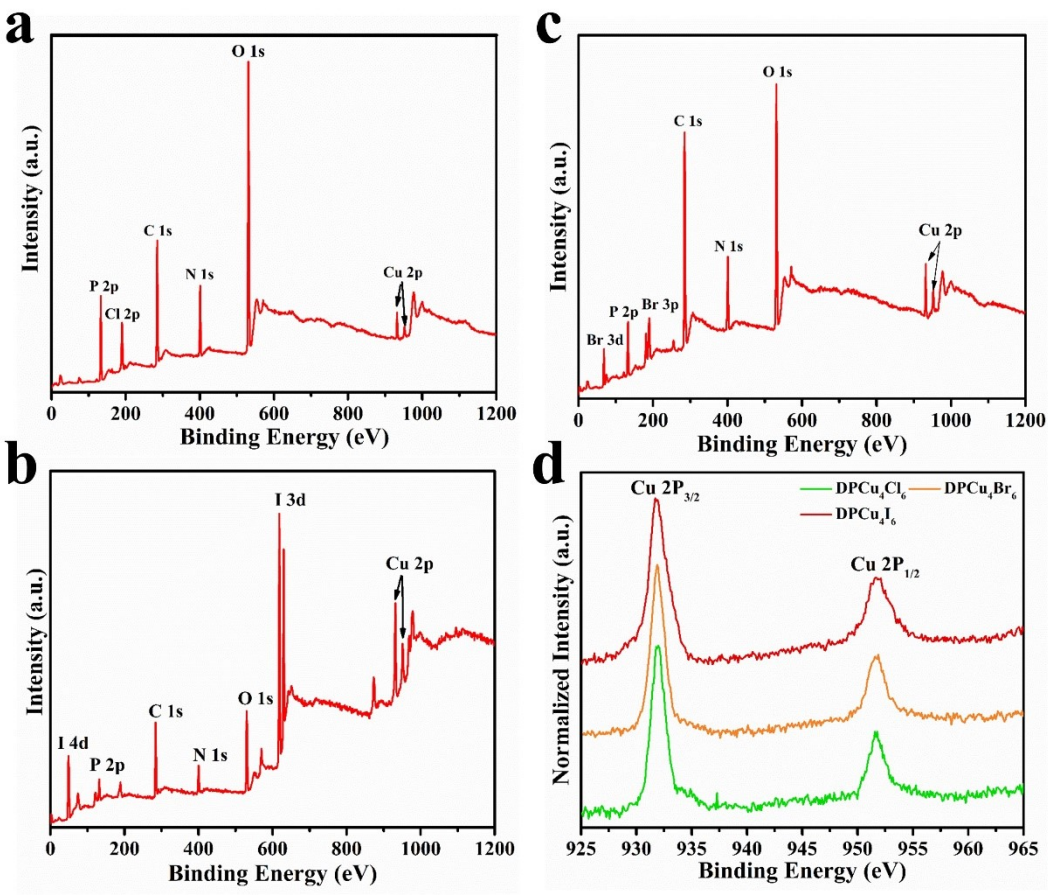


**Figure S5.** XPS spectra of (a) $DPCu_4Cl_6$, (b) $DPCu_4Br_6$ and (c) $DPCu_4I_6$ single crystals and the high-resolution spectra of (d) Cu 2p.

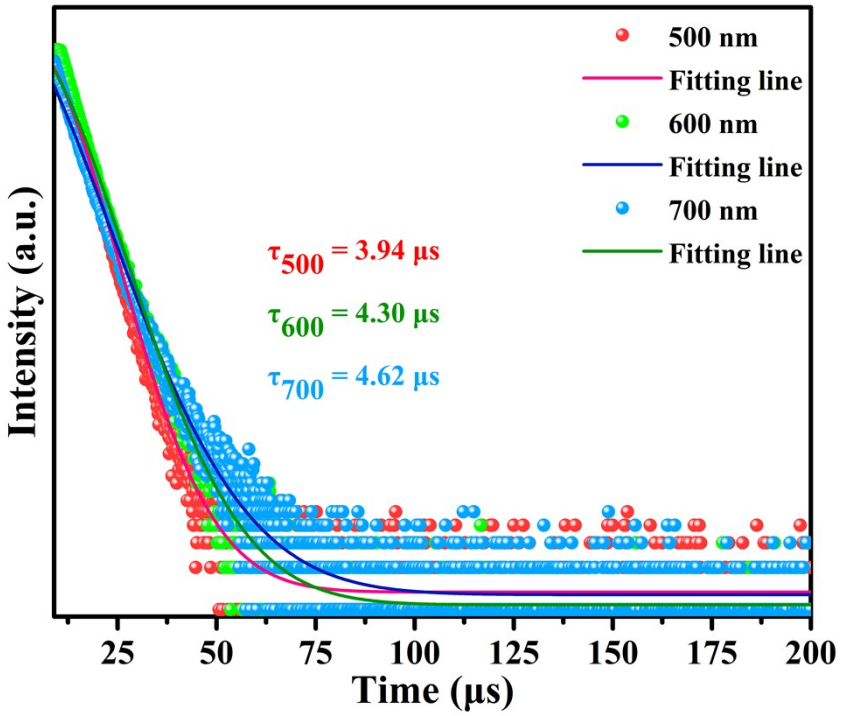


**Figure S6.** Time-resolved PL spectra of $DPCu_4I_6$ single crystals at RT monitored at different excitation wavelengths.

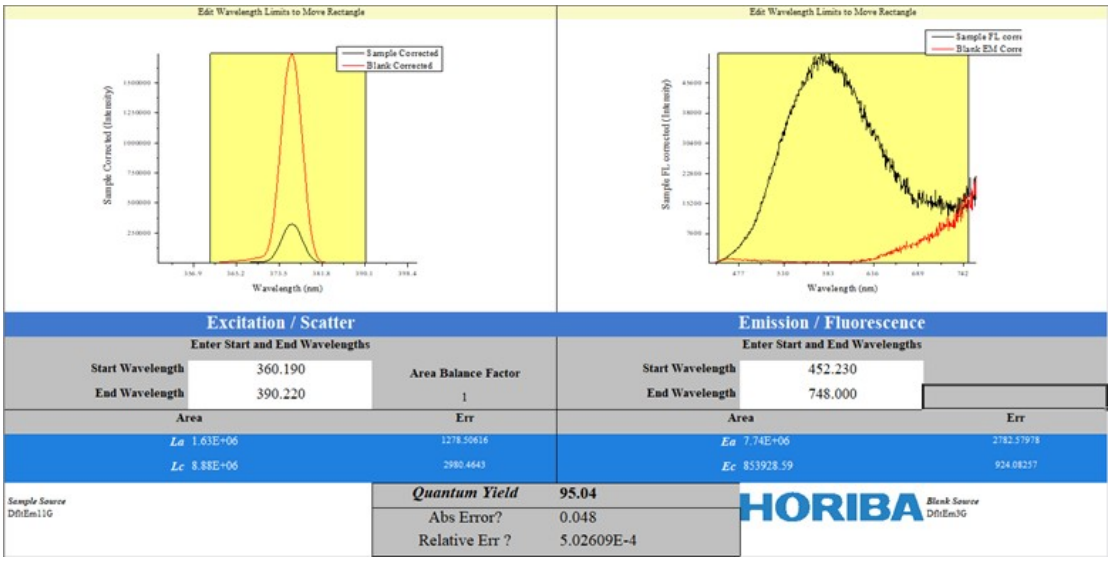


**Figure S7.** The PLQY of $DPCu_4Br_6$ single crystals.

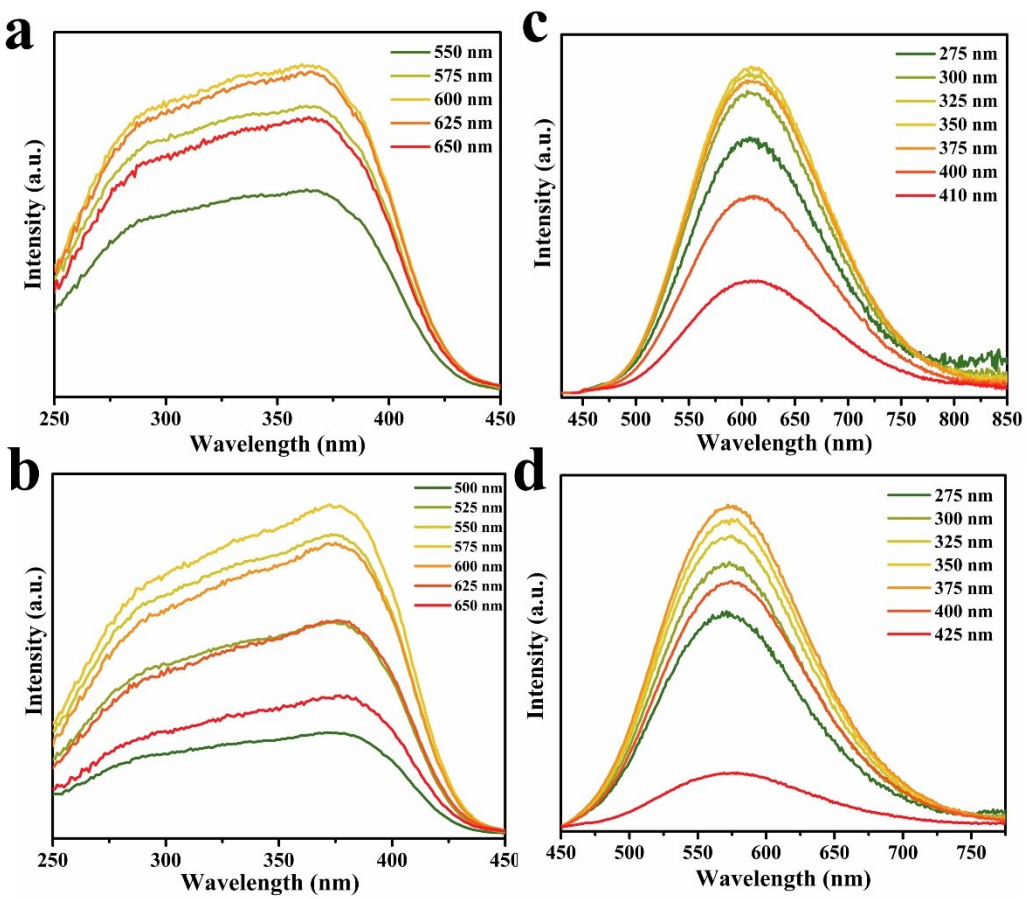


**Figure S8.** Emission-wavelength dependent PLE spectra of (a) DPCu4Cl6 and (b) $DPCu_4Br_6$ crystals at room temperature. Excitation-wavelength dependent PL spectra of (c) DPCu4Cl6 and (d) $DPCu_4Br_6$ crystals at room temperature.

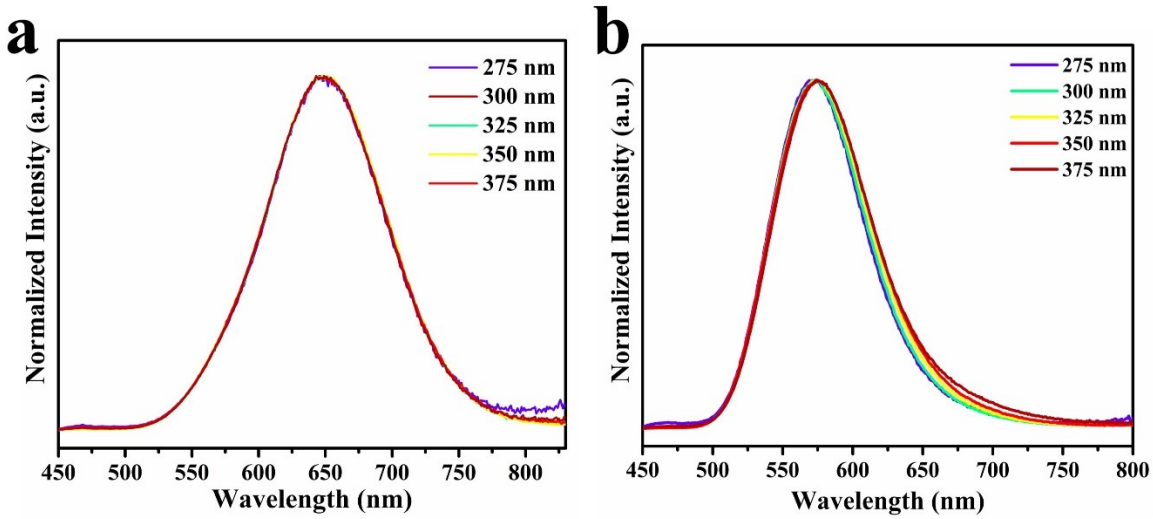


**Figure S9.** Normalized Excitation-wavelength dependent PL spectra of (a) $DPCu_4Cl_6$ and (b) $DPCu_4Br_6$ crystals at 80 K.

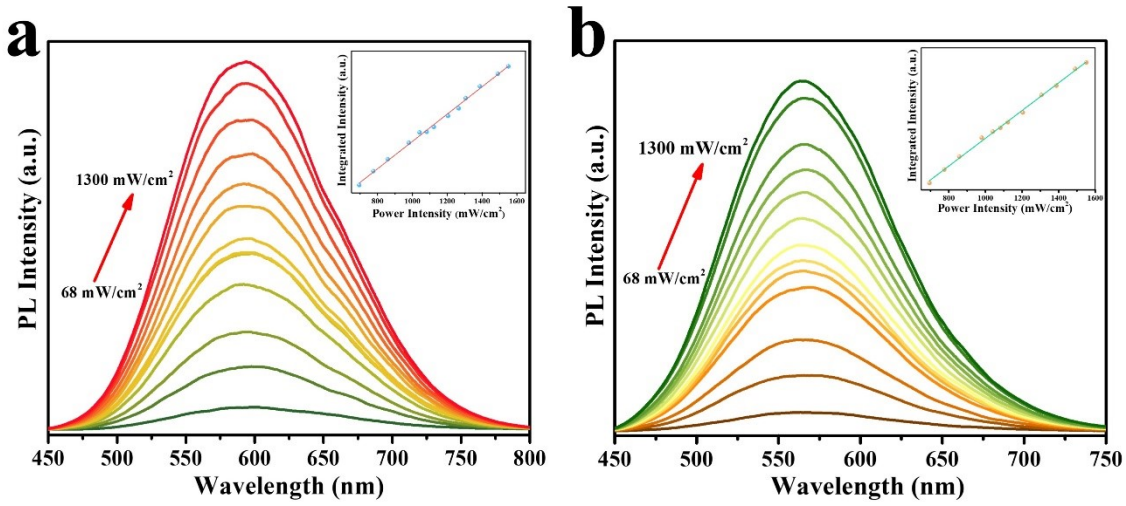


**Figure S10.** PL spectra of (a) $DPCu_4Cl_6$ and (b) $DPCu_4Br_6$ recorded by varying the excitation power density. Inset shows the plots of PL intensity as a function of excitation power density

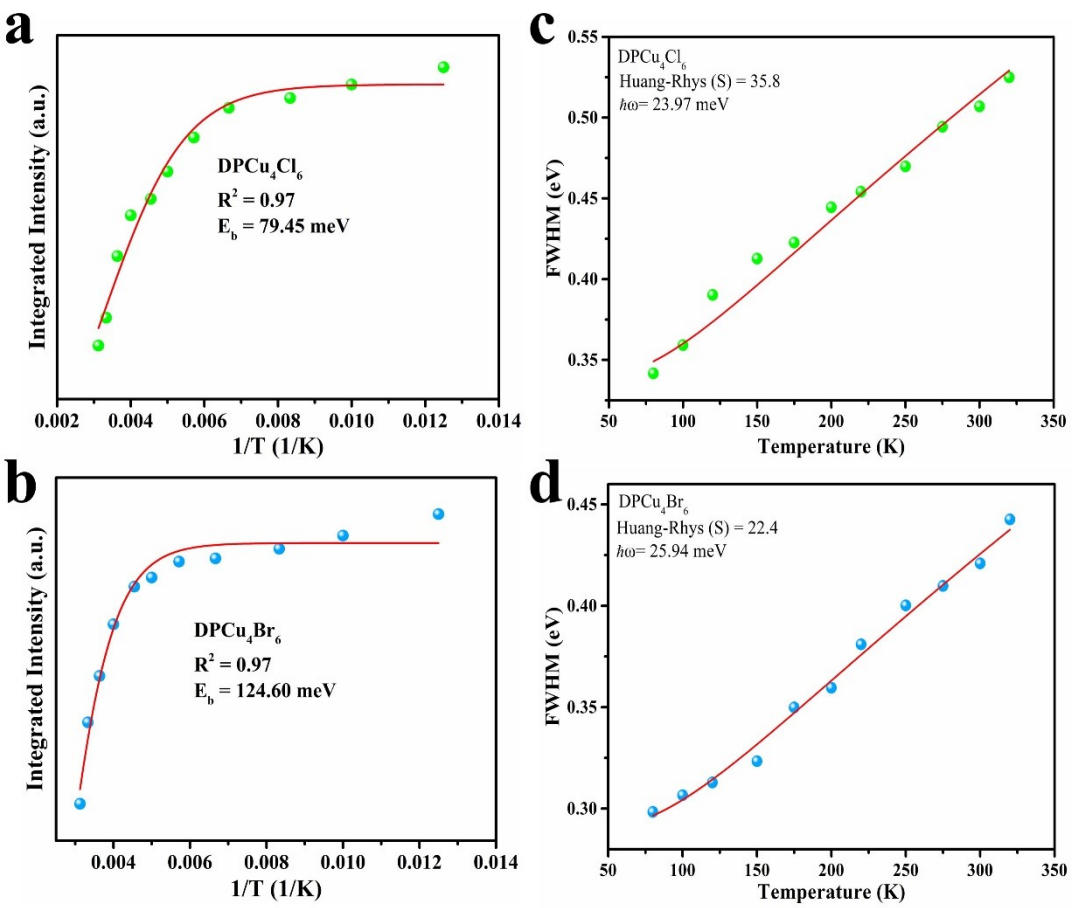


**Figure S11.** Fitting results of the integrated PL intensity as a function of temperature for (a) $DPCu_4Cl_6$ and (b) $DPCu_4Br_6$. Fitting results of the FWHM as a function of temperature for (c) $DPCu_4Cl_6$ and (d) $DPCu_4Br_6$.

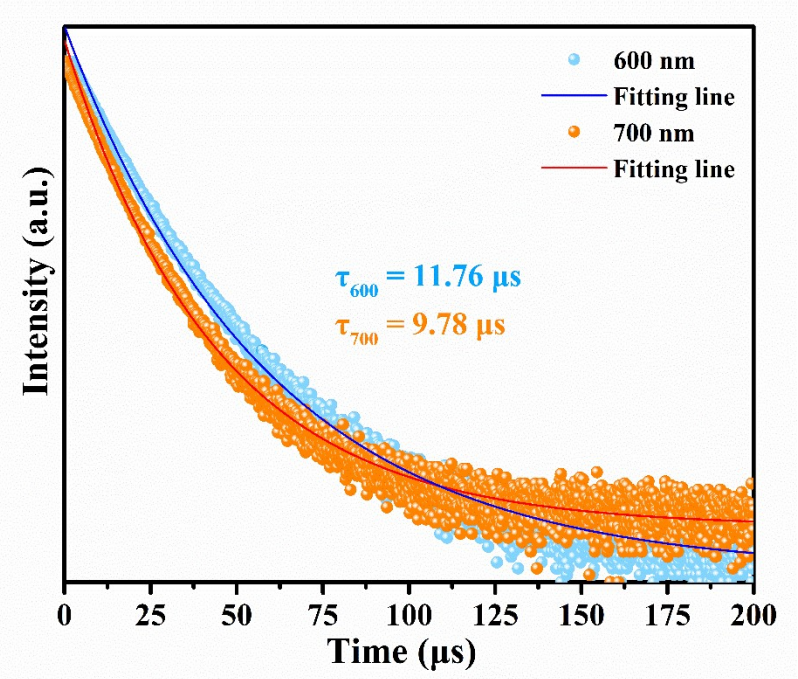


**Figure S12.** Time-resolved PL spectra of $DPCu_4I_6$ single crystals at 80 K monitored at 600 and 700 nm.

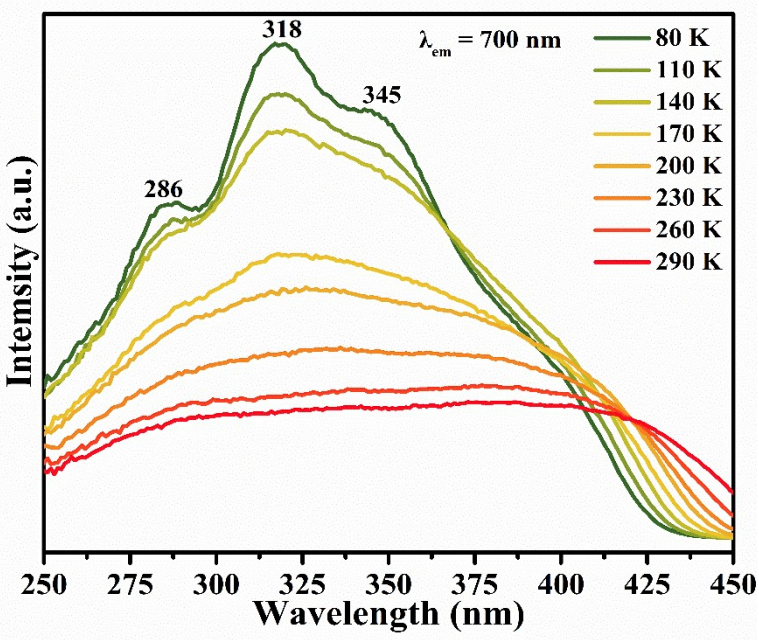


**Figure S13.** Temperature-dependent PLE spectra of $DPCu_4I_6$ single single crystals monitored at 700 nm.

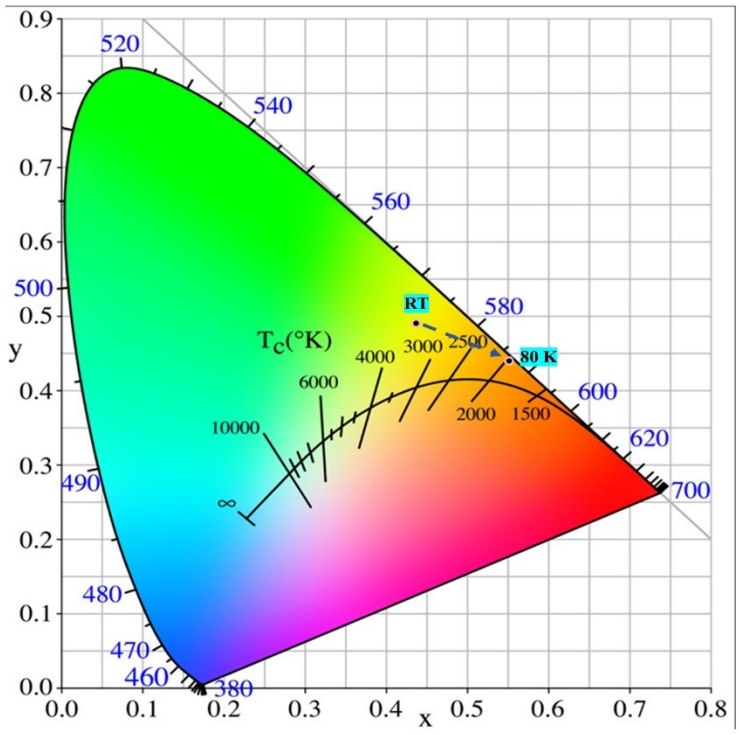


**Figure S14.** The corresponding CIE diagram of $DPCu_4I_6$ single crystals at room temperature and 80 K.

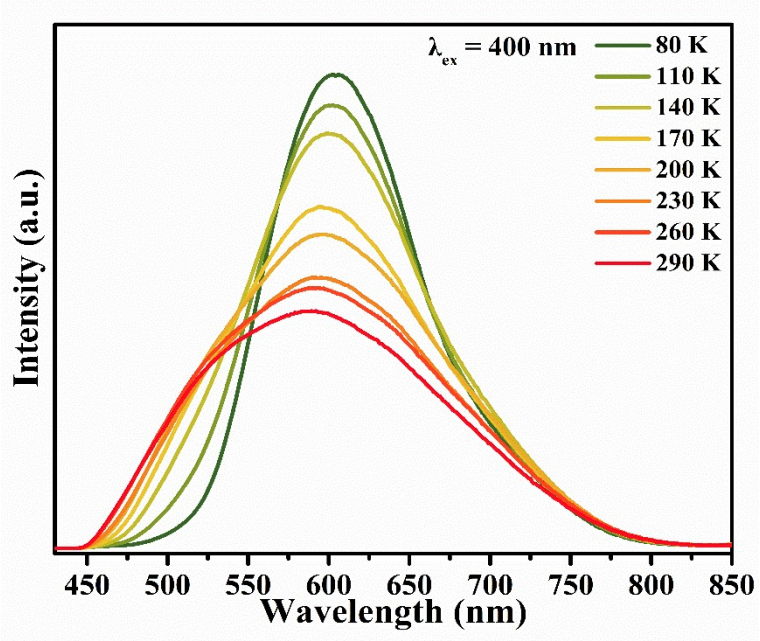


**Figure S15.** Temperature-dependent PL spectra of $DPCu_4I_6$ single crystals under 400 nm excitation

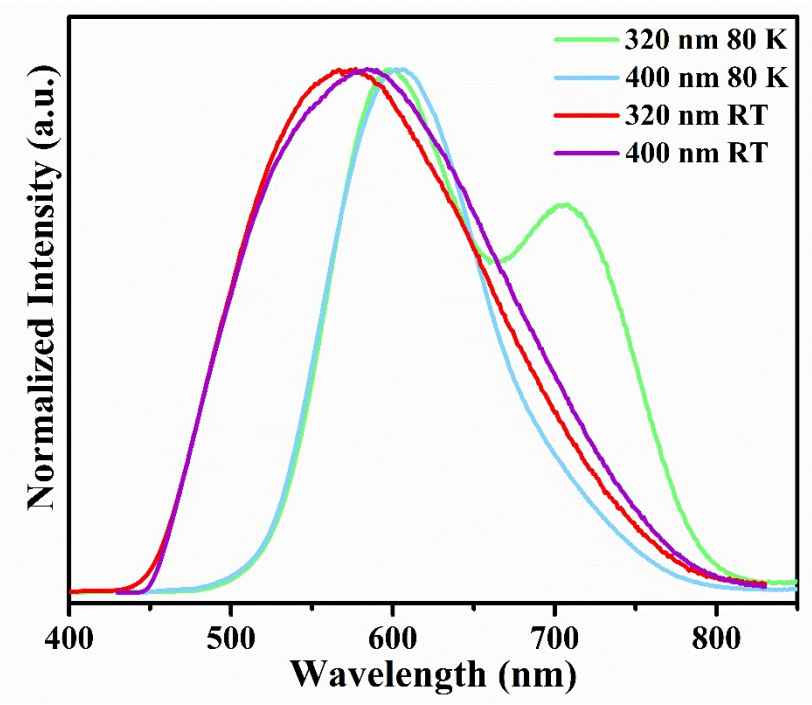


**Figure S16.** PL spectra of DPCu4I6 under 320 nm and 400 nm excitation at 80 K and RT.

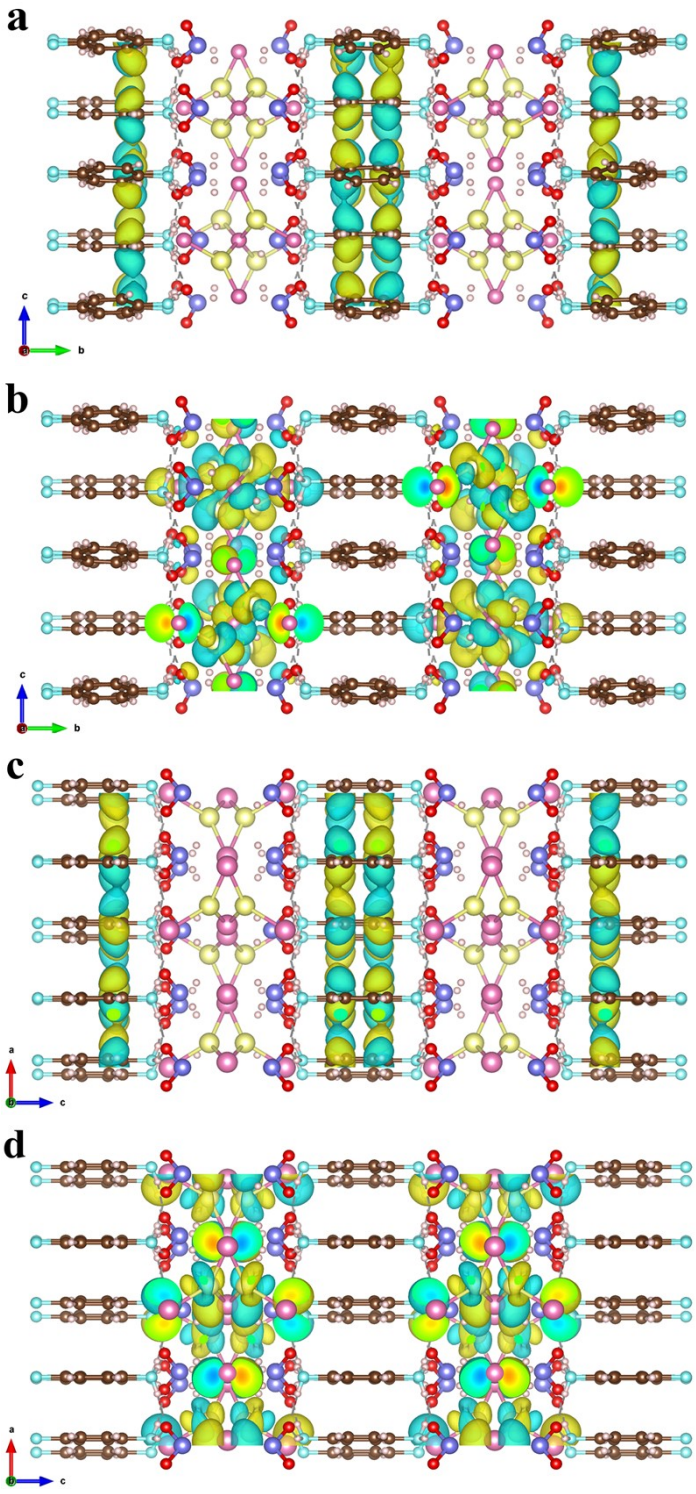


**Figure S17.** Charge densities of the (a) CBM and (b) VBM for $DPCu_4Cl_6$. Charge densities of the (c) CBM and (d) VBM for $DPCu_4I_6$.

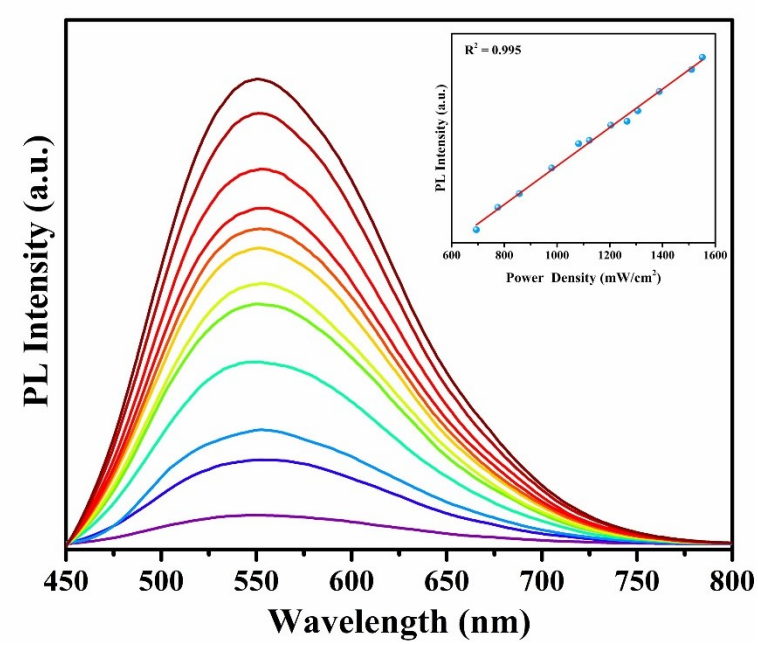


**Figure S18.** PL spectra of $DPCu_4I_6$ recorded by varying the excitation power density. The inset shows that the integrated broadband PL intensity of $DPCu_4I_6$ is linearly related to the excitation power.

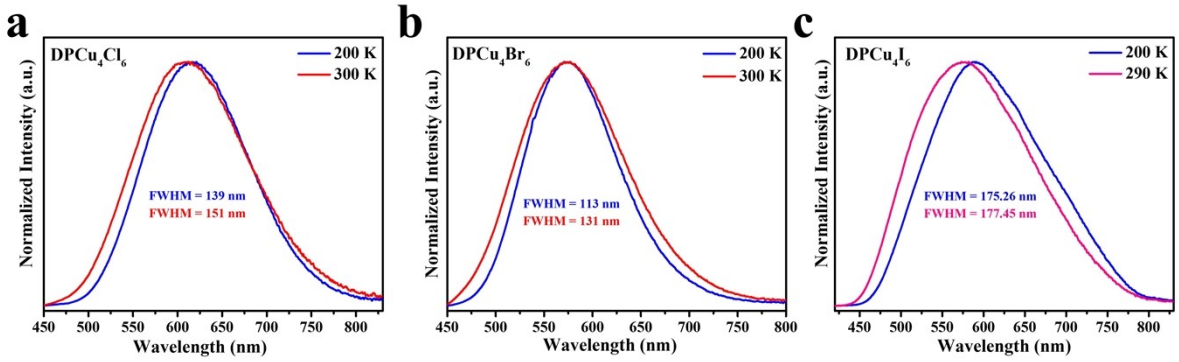


**Figure S19.** PL spectra of $DPCu_4Cl_6$ (a) $DPCu_4Br_6$ (b) and at 200 K and 300 K. (c) PL spectra of $DPCu_4I_6$ (c) and at 200 K and 290 K.

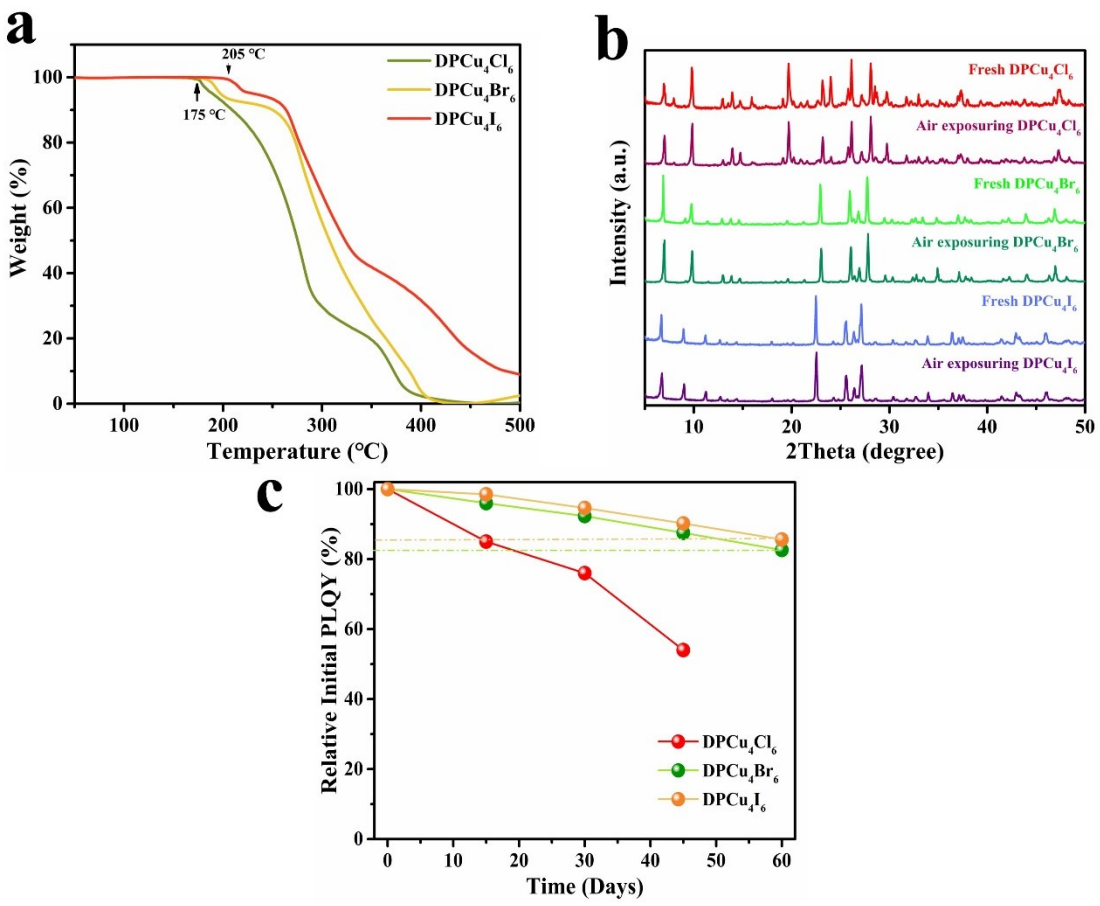


**Figure S20.** (a) Thermogravimetric curves for $DPCu_4X_6$ (X = Cl, Br, I). (b) PXRD patterns of $DPCu_4X_6$ (X = Cl, Br, I) before and after exposure to atmospheric environment with ～75 % relative humidity (30 days for $DPCu_4Cl_6$ and two months for $DPCu_4Br_6$ and $DPCu_4I_6$).(c) The PL stability of $DPCu_4X_6$ (X = Cl, Br, I) single crystals at different times within two months.

**Table S1.** The crystal structure parameters of $DPCu_4X_6$ (X = Cl, Br, I) single crystals.

| **Chemical formula** | **$C_{12}H_{26}Cl_3Cu_2N_4O_6P_3$** | **$C_{12}H_{26}Br_3Cu_2N_4O_6P_3$** | **$C_{12}H_{26}I_3Cu_2N_4O_6P_3$** |
|---|---|---|---|
| **Abbreviation** | DPCu4Cl6 | $DPCu_4Br_6$ | $DPCu_4I_6$ |
| **Formula weight** | 648.71 | 782.09 | 917.01 |
| **Temperature/K** | 173.00 | 173.00 | 193.00 |
| **Crystal system** | orthorhombic | tetragonal | tetragonal |
| **Space group** | Ccce | $I4_1/acd$ | P4/m |
| ***a*/Å** | 13.6165(6) | 13.6690(6) | 13.8592(5) |
| ***b*/Å** | 25.2859(10) | 13.6690(6) | 13.8592(5) |
| ***c*/Å** | 13.6152(5) | 13.6152(5) | 13.1579(7) |
| **α/°** | 90 | 90 | 90 |
| **β/°** | 90 | 90 | 90 |
| **γ/°** | 90 | 90 | 90 |
| **Volume/Å3** | 4687.8(3) | 9588.8(11) | 2527.3(2) |
| **ρcalc(g/cm3)** | 1.838 | 2.167 | 2.410 |
| **μ/$mm^{-1}$** | 2.398 | 7.011 | 5.572 |
| **F(000)** | 2624.0 | 6112.0 | 1720.0 |
| **2Θ range for data collection/°** | 5.984 to 55.022 | 4.504 to 55.016 | 4.268 to 55.198 |
| **Independent reflections** | 2696 [$R_{int}$ = 0.0357, $R_{sigma}$ = 0.0200] | 2759 [$R_{int}$ = 0.0788, $R_{sigma}$ = 0.0351] | 3007 ($R_{int}$ = 0.0571, $R_{sigma}$ = 0.0369) |
| **Final R indexes [I>=2σ (I)]** | $R_1$ = 0.0271, $wR_2$ = 0.0620 | $R_1$ = 0.0323, $wR_2$ = 0.0797 | $R_1$ = 0.1364, wR2 = 0.3418 |
| **Final R indexes [all data]** | $R_1$ = 0.0319, $wR_2$ = 0.0645 | $R_1$ = 0.0402, $wR_2$ = 0.0840 | $R_2$ = 0.1380, wR2 = 0.3424 |

**Table S2.** Hydrogen-bond geometry in $DPCu_4X_6$ (X = Cl, Br, I) SCs (Å, ˚)

| **Donor --- H....Acceptor** | **d (D - H)/Å** | **d (H... A)/Å** | **d (D... A)/Å** | **∠D – H ... A/°** |
|---|---|---|---|---|
| **$DPCu_4Cl_6$** | | | | |
| N1--H1A…O2 | 0.91 | 1.83 | 2.713(2) | 163 |
| N1--H1B…O3 | 0.91 | 1.86 | 2.769(2) | 172 |
| N1--H1C…O1 | 0.91 | 1.87 | 2.740(2) | 160 |
| N2--H2A…O3 | 0.91 | 1.83 | 2.738(2) | 173 |
| N2--H2B…O1 | 0.91 | 1.89 | 2.778(2) | 166 |
| N2--H2C…O2 | 0.91 | 1.96 | 2.815(2) | 155 |
| C6--H6…O2 | 0.95 | 2.54 | 3.289(3) | 136 |
| **$DPCu_4Br_6$** | | | | |
| N1--H1A…O3 | 0.91 | 1.92 | 2.777(4) | 157 |
| N1--H1B…O1 | 0.91 | 1.85 | 2.755(4) | 174 |
| N1--H1C…O2 | 0.91 | 1.84 | 2.732(4) | 165 |
| N2--H2A…O3 | 0.91 | 1.88 | 2.769(4) | 167 |
| N2--H2B…O2 | 0.91 | 1.97 | 2.824(4) | 156 |
| N2--H2C…O1 | 0.91 | 1.81 | 2.723(4) | 175 |
| C2--H2…O1 | 0.95 | 2.55 | 3.265(5) | 132 |
| C3--H3…Br2 | 0.95 | 2.88 | 3.723(4) | 149 |
| C6--H6…O2 | 0.95 | 2.55 | 3.303(5) | 136 |
| **$DPCu_4I_6$** | | | | |
| N1--H1A…O3 | 0.91 | 1.92 | 2.80(2) | 162 |
| N1--H1B…O1 | 0.91 | 1.81 | 2.72(2) | 171 |
| N1--H1C…O2 | 0.91 | 2.01 | 2.89(3) | 162 |
| N2--H2A…O2 | 0.91 | 1.87 | 2.73(2) | 156 |
| N1--H2B…O1 | 0.91 | 1.87 | 2.75(2) | 162 |

| | | | | |
|---|---|---|---|---|
| N2--H2C…O3 | 0.91 | 1.97 | 2.86(2) | 168 |
| C0--H0…I1 | 0.96 | 2.94 | 3.81(5) | 151 |
| C3--H3…O1 | 0.95 | 2.55 | 3.26(5) | 131 |
| C5--H5…O3 | 0.95 | 2.47 | 3.21(6) | 135 |

**Table S3.** A comparison of the PL properties between $DPCu_4X_6$ and other low-energy emissive Cu(I)-based compounds.

| Compounds | PLE peak (nm) | PL peaks (nm) | FWHM (nm) | PLQY (%) | Ref |
|---|---|---|---|---|---|
| $(Bmpip)_2Cu_2Br_4$ | 320 | 620 | 158 | 48.2 | 4 |
| $(PTMA)_3Cu_3I_6$ | 358 | 614 | 160 | 80.3 | 5 |
| K(18-crown-6)$Cu_2Br_3$ | 375 | 668 | - | 53 | 6 |
| $CsCu_2I_3$ | 330 | 550 | 115 | 15 | 7 |
| $(R\text{-}MBA)_4Cu_4I_4$ | 360 | 630 | 118 | 52.8 | 8 |
| $(S\text{-}MBA)_4Cu_4I_4$ | 360 | 630 | 118 | 59.7 | |
| $(DTA)_2Cu_2I_4$ | 320 | 533 | 180 | 60 | 9 |
| KCB-DMSO | 382 | 678 | 157 | 74.8 | 10 |
| RCB-DMSO | 396 | 688 | 166 | 74.5 | |
| ((S)-(-)-α-PEA)$_4Cu_4I_4$ | 346 | 635 | 146 | 73.6 | 11 |
| ((R)-(+)-α-PEA)$_4Cu_4I_4$ | 346 | 635 | 145 | 67.8 | |
| $[KC2]_2[Cu_4I_6]$ | 400 | 545 | 145 | 97.8 | 12 |
| **$DPCu_4Cl_6$** | **364** | **612** | **148** | **89.76** | **This work** |
| **$DPCu_4Br_6$** | **377** | **575** | **123** | **95.04** | |
| **$DPCu_4I_6$** | **292** | **575** | **185** | **93.52** | |

**Table S4.** Summary of the optical properties of some single-component perovskite-based WLED reported in recent years.

| Materials | PLQY (%) | CIE | CRI | CCT (K) | Ref |
|---|---|---|---|---|---|
| $(C_6H_7ClN)CdCl_3$ | 12.3 | (0.3433, 0.3044) | 83.7 | 5214 | 13 |
| $BAPPIn_{1.996}Sb_{0.004}Cl_{10}$ | 44.0 | | 73.9 | 6206 | 14 |
| $[(NH_4)(18\text{-crown-}6)]_2SbCl_5\cdot DMF$ | 37 | (0.46, 0.36) | 76 | 2270 | 15 |
| [Rb(18-crown-6)]2SbCl5·DMF | 54 | (0.43, 0.34) | 74 | 2513 | 15 |
| $(C_{16}H_{36}N)CuI_2$ | 54.3 | (0.28 0.30) | 78 | | 16 |
| $(TTA)_2SbCl_5$ | 68 | (0.46, 0.36) | 84 | 2248 | 17 |
| $PA_6InCl_9$:2.5%Sb | 99.3 | (0.39, 0.41) | 86 | 3983 | 18 |
| $Na_4(18\text{-crown-}6)_5In_2Cu_4Br_{14}\cdot 8H_2O$ | 97.2 | (0.37, 0.42) | 75 | 4429 | 6 |
| $(2\text{-FPMA})_2PbBr_4$ | 5 | (0.342, 0.361) | 89 | 5139 | 19 |
| $(2\text{-ClPMA})_2PbBr_4$ | 32 | (0.300, 0.330) | 86 | 7215 | 19 |
| $(2\text{-BrPMA})_2PbBr_4$ | 15 | (0.312, 0.338) | 88 | 6478 | 19 |
| γ-MPAPB | 6.85 | (0.22, 0.23) | 85 | 53281 | 20 |
| $(Ph_3MeP)_2Cu_4I_6$ | 69 | (0.41, 0.39) | 88 | 3500 | 21 |
| $(TPA)CuI_2$ | 84.4 | (0.31, 0.33) | 91.3 | 6574 | 22 |
| $(C_5H_7N_2)_2HgBr_4\cdot H_2O$ | 14.87 | (0.34, 0.38) | 87 | 5206 | 23 |
| $(C_5H_7N_2)_2ZnBr_4$ | 19.18 | (0.25, 0.26) | 96 | 11630 | 23 |
| $(C_8NH_{12})_6InBr_9\cdot H_2O$:0.1%Sb | 23.36 | (0.400, 0.361) | 84 | 3347 | 24 |
| $[H_2DABCO][Ag_2Br_4(DABCO)]$ | 6.7 | (0.28, 0.32) | 85 | 8375 | 25 |
| $[DTHPE]_2Pb_3Cl_{10}$ | 19.45 | (0.25, 0.29) | 81 | 14300 | 26 |
| **$DPCu_4I_6$** | **93.52** | **(0.36, 0.35)** | **85** | **4415** | **This work** |

## References


1 G. Kresse and J. Furthmuller, *Comput. Mater. Sci.*, 1996, **6**, 15-50.

2 G. Kresse and D. Joubert, *Phys. Rev. B*, 1999, **59**, 1758-1775.

3 J. P. Perdew, K. Burke and M. Ernzerhof, *Phys. Rev. Lett.*, 1997, **78**, 1396-1396.

4 T. T. Xu, Y. Y. Li, M. Nikl, R. Kucerkova, Z. Y. Zhou, J. Chen, Y. Y. Sun, G. D. Niu, J. Tang, Q. Wang, G. H. Ren and Y. T. Wu, *ACS Appl. Mater. Interfaces*, 2022, **14**, 14157-14164.

5 L. Y. Lian, T. J. Zhang, H. Y. Ding, P. Zhang, X. W. Zhang, Y. B. Zhao, J. B. Gao, D. L. Zhang, Y. S. Zhao and J. B. Zhang, *ACS Mater. Lett.*, 2022, **4**, 1446-1452.

6 X. Liu, Y. Li, L. Zhou, M. Li, Y. Y. Zhou and R. X. He, *Adv. Optical. Mater.,* 2022, **10**, 2200944.

7 L. T. Wang, Z. Z. Ma, F. Zhang, M. Wang, X. Chen, D. Wu, Y. T. Tian, X. J. Li and Z. F. Shi, *J. Mater. Chem. C*, 2021, **9**, 6151-6159.

8 L. Yao, G. D. Niu, J. Z. Li, L. Gao, X. F. Luo, B. Xia, Y. H. Liu, P. P. Du, D. H. Li, C. Chen, Y. X. Zheng, Z. W. Xiao and J. Tang, *J. Phys. Chem. Lett.*, 2020, **11**, 1255-1260.

9 F. Liu, D. Mondal, K. Zhang, Y. Zhang, K. K. Huang, D. Y. Wang, W. S. Yang, P. Mahadevan and R. G. Xie, *Mater. Adv.*, 2021, **2**, 3744-3751.

10 Y. Y. Li, Z. C. Zhou, F. K. Sheong, Z. S. Xing, R. Lortz, K. S. Wong, H. H. Y. Sung, I. D. Williams and J. E. Halpert, *ACS Energy Lett.*, 2021, **6**, 4383-4389.

11 S. F. Fang, H. N. Li, Y. L. Xie, H. X. Li, Y. Wang and Y. M. Shi, *Small*, 2021, **17**, 2103831.

12 S. Li, J. Xu, Z. G. Li, Z. C. Zeng, W. Li, M. H. Cui, C. C. Qin and Y. P. Du, *Chem. Mater.*, 2020, **32**, 6525-6531.

13 H. Xu, Z. Zhang, X. Dong, L. Huang, H. Zeng, Z. Lin and G. Zou, *Inorg. Chem.*, 2022, **61**, 4752-4759.

14 J. H. Wei, J. F. Liao, L. Zhou, J. B. Luo, X. D. Wang and D. B. Kuang, *Sci. Adv.*, 2021, **7**, eabg3989.

15 J. Xu, S. Li, C. Qin, Z. Feng and Y. Du, *, J. Phys. Chem. C*, 2020, **124**, 11625-

11630.

16 L. Y. Lian, P. Zhang, G. J. Liang, S. Wang, X. Wang, Y. Wang, X. W. Zhang, J. B. Gao, D. L. Zhang, L. Gao, H. S. Song, R. Chen, X. Z. Lan, W. X. Liang, G. D. Niu, J. Tang and J. B. Zhang, *ACS Appl. Mater. Interfaces*, 2021, **13**, 22749-22756.

17 Z. Li, Y. Li, P. Liang, T. Zhou, L. Wang and R. J. Xie, *Chem. Mater.*, 2019, **31**, 9363-9371.

18 S. W. Feng, Y. J. Ma, S. Q. Wang, S. S. Gao, Q. Q. Huang, H. Y. Zhen, D. P. Yan, Q. D. Ling and Z. H. Lin, *Angew. Chem. Int. Ed.*, 2022, **61**, e202116511.

19 M. M. Zhang, L. L. Zhao, J. H. Xie, Q. Zhang, X. Y. Wang, N. Yaqoob, Z. M. Yin, P. Kaghazchi, S. Zhang, H. Li, C. F. Zhang, L. Wang, L. J. Zhang, W. G. Xu and J. Xing, *Nat. Commun.*, 2021, **12**, 4890.

20 Y. Li, C. Ji, L. Li, S. Wang, S. Han, Y. Peng, S. Zhang and J. Luo, *Inorg. Chem. Front.*, 2021, **8**, 2119-2124.

21 P. Fu, S. Geng, R. Mi, R. Wu, G. Zheng, B. Su, Z. Xia, G. Niu, J. Tang and Z. Xiao, *Energy Environ. Mater.*, e12518. https://doi.org/10.1002/eem2.12518.

22 L. Lian, S. Wang, H. Ding, G. Liang, Y. B. Zhao, H. Song, X. Lan, J. Gao, R. Chen, D. Zhang and J. Zhang, *Adv. Optical. Mater.*, 2022, **10**, 2101640.

23 A. Yangui, R. Roccanova, T. M. McWhorter, Y. T. Wu, M. H. Du and B. Saparov, *Chem. Mater.*, 2019, **31**, 2983-2991.

24 Z. Y. Li, G. M. Song, Y. Li, L. Wang, T. L. Zhou, Z. S. Lin and R. J. Xie, *J. Phys. Chem. Lett.*, 2020, **11**, 10164-10172.

25 C. Sun, Y.-H. Guo, Y. Yuan, W. X. Chu, W. L. He, H. X. Che, Z. H. Jing, C. Y. Yue and X. W. Lei, *Inorg. Chem.*, 2020, **59**, 4311-4319.

26 J. Q. Zhao, C. Sun, M. Yue, Y. Meng, X.-M. Zhao, L.-R. Zeng, G. Chen, C. Y. Yue and X. W. Lei, *Chem. Commun.*, 2021, **57**, 1218-1221.